Preferred citation: B. Zhao, R. Pelton and V. Bartzoka. Peeling pressure sensitive tape from paper. In **Advances in Paper Science and Technology**, *Trans. of the XIIIth Fund. Res. Symp. Cambridge, 2005*, (S.J. I'Anson, ed.), pp 827–850, FRC, Manchester, 2018. DOI: 10.15376/frc.2005.2.827.

PEELING PRESSURE SENSITIVE TAPE FROM PAPER

Boxin Zhao, Robert Pelton and Vasiliki Bartzoka

Department of Chemical Engineering, McMaster University, Hamilton, Ontario, Canada, L8S 4L7

ABSTRACT

The ability of adhesives to bond paper and paperboard is critical for most packaging and converting operations. Despite the huge body of literature describing both paper and adhesives technologies, there are only a few research papers describing paper/adhesive interactions. Described herein are the results of a systematic investigation of pressure sensitive adhesive (PSA) peeling from paper. The peel force versus peel distance curve depends upon the failure mode. A constant force is observed when the PSA cleanly separates from paper (i.e. interfacial failure) at low peel rate. By contrast, at high peeling rates, in the paper failure domain, the peel force climbs to a maximum and then relaxes to a steady-state value. The maximum peel force, which we call the peak force, corresponds to the fracture of the top layer of fibres during the initiation of paper delamination whereas the steady-state peel force occurs during the propagation of paper delamination.

To characterize the range of behaviors it is necessary to conduct a series of peeling experiments over an extended range of peel rates. The results are best analyzed by plotting the peak peel force versus the peel rate on logarithmic axes giving what we call a peel map. For a broad range of tape/paper combinations, peel maps have similar shapes. The interfacial failure domain consists of a linear segment with a positive slope. This line intersects with a horizontal line segment at higher peel rates, corresponding to the paper failure domain.

Principal component analysis, a multivariate statistical analysis, of a large set of peel maps was used to reveal the influence of paper properties on peeling. The peak peel forces in the paper failure domain correlated with standard paper properties linked to z-directional strength. The slopes of the peel maps in the interfacial domain were independent of paper properties but were sensitive to adhesive rheology. The absolute location of the interfacial segment of the peel map mainly was sensitive to the chemical composition of the paper surface and secondarily related to surface roughness. Water contact angles on paper were not good predictors of adhesion. Finally, we illustrate the utility of peak peel force in the paper failure domain as a measure of paper surface strength.

INTRODUCTION

Corrugated box construction, xerography, paper splicing, address label application and the lamination of plastic films to paperboard all depend upon polymer adhesion to paper and paper board. Xerographic toners and lamination films are heated during contact with paper so the thermoplastic polymers can flow against the paper. By contrast, box construction, paper splicing and address label applications employ adhesives which promote adhesion between paper surfaces. Over the past several years, 3M Canada and the Canadian government have funded a project at McMaster University aimed at revealing the details of pressure sensitive adhesive tape (PSA) interactions with paper surfaces. The goal of this paper is to present new results linking paper surface chemistry to PSA adhesion. Some highlights of our work recently published in the adhesion and material science journals are also summarized to provide a context for the new results.

Much of our experimentation involved peeling tapes from paper surfaces. Tape peeling from other surfaces has been extensively discussed in the literature and the main conclusions from the literature are now summarized. Following this, a brief literature review on paper adhesion is given with emphasis on the effects of paper surface chemistry and paper structure.

The peel test

Peel testing and shear strength measurements (usually a shear creep test) are the primary industrial methods used to evaluate PSA performance [1]. Shear

tests give a measure of the PSA cohesive strength whereas peeling is sensitive to both cohesive and adhesive interactions. The challenge for PSA formulators is simultaneously to achieve high values of "peel" and "shear".

Peel tests are usually performed with a laminate consisting of a strong flexible backing such as polyester film stuck to a stainless steel plate with layer of PSA (for example see ASTM D93). Peel rate and peel angle are the controllable experimental variables – these are discussed below. Peel force versus peeling distance is the measured quantity together with an assessment of the locus of failure. Peel forces are usually reported as the total force divided by the sample width. In addition to peel force, knowledge of the locus of failure is also important. PSA cohesive or interfacial failure are the only possibilities with laminates based on stainless steel and a strong backing film. By contrast, peeling from paper often leads to some form of paper failure. Peel rate is a critical parameter [2]. As children we learned that if one peels a PSA slowly from paper, clean interfacial failure is obtained whereas at high rate, the paper fails. Because PSAs are viscoelastic materials, the peel force increases with peel rate over a broad range of peel rates [2].

Peel forces always vary with peel angle. Most measurements are made at a superficial peel angle of 90 or 180 degrees – the actual angle over the peeling front is poorly defined in most experimental setups. Kaelble proposed that peel should vary inversely with $1 - \cos \theta$ where θ is the peel angle [3]; however, most systems display more complex behavior [4]. The origin of the complexity is that part of the work of peeling involves the irreversible work of bending the adhesive and the backing. The importance of bending was emphasized by Yelon and coworkers who analyzed paper delamination in peel. They reported paper delamination peel forces as a function of peel angle. In addition, they measured the minimum radius of curvature of the peeled paper layer. The true delamination force was obtained by extrapolating the measured forces to a value corresponding to zero curvature [5, 6, 7].

Peeling experiments are attractive because they are easy to perform and they yield reproducible results. From a fundamental perspective peeling is very complex. A typical PSA peel front spans about one mm. As the tape lifts away from the surface, the adhesive is present as long strands the PSA technologists call "fibrils". Behind the fibrils, where the tape first starts to lift, vapor bubbles appear in the adhesive layer, a process called cavitation in the adhesion literature [8]. In spite of this complexity, there are approximate analytical models of the stress distribution across a PSA peeling front [9, 10] as well as a recent finite element simulation of peeling [11].

To circumvent the complexities of peeling, a number of investigators have measured the adhesion between rubber caps, coated with PSA, against hard

surfaces [12, 13]. In this technique, the contact area is measured as a function of pressure and the corresponding adhesion energy is calculated with JKR contact mechanics theory [14]. Li et al. [15] showed that for a PSA tape adhesion to a glass plate coated with the same PSA, the energy release rate(i.e. the practical adhesion energy), G, approached the thermodynamic work of adhesion at very low crack growth rates. Furthermore, the peel work values could be predicted by extrapolating G to high strain rates using the following equation;

$$G = G_o\left(1 + \left(\frac{v}{v^*}\right)^n\right) \tag{1}$$

where $\boldsymbol{G_o}$ is the energy release rate at infinitely low crack growth rate which is equivalent to the thermodynamic work of adhesion for pure interfacial failure; v is the crack growth rate; v* is a critical separation rate and $\boldsymbol{n}$ is a fitting parameter which reflects the adhesive rheology.

The influence of paper surface chemistry on adhesion

The thermodynamic work of adhesion, $\boldsymbol{W}$ between a paper surface and a layer of adhesive is given in Equation (2) as a function of the surface energy of the paper, γ_P, the surface energy of the adhesive, γ_A, and the adhesive/paper interfacial energy γ_{PA}.

$$W = \gamma_P + \gamma_A - \gamma_{PA} \tag{2}$$

Although it is unlikely that $\boldsymbol{W}$ will be useful in predicting practical adhesion, Equation (2) is important because it illustrates the relationship between ideal adhesion and surface energy which, in turn, is dependent upon surface chemistry. There are many publications describing the determination of paper surface energy from contact angle measurements [16] and inverse gas chromatography [17]. However, only a few attempts have been made to link paper surface energy to adhesion – these are summarized in Borch's review [18]. Swanson and Becher reported poor adhesion between paper and polyethylene when the critical surface tension of paper was lower than that of polyethylene [19]. Borch showed that the adhesion of thermoplastic toners to paper increased with the surface energy of paper estimated from contact angle measurements and inverse gas chromatography [18, 20]. Similar conclusions were reached by Gervason and coworkers who showed that the delamination force for polyethylene-paper laminates increased with paper surface energy for a series of sized papers [21].

Many adhesion studies involving plastic film/paper laminates have been published in which the paper surface composition and thus the paper surface energy was varied but not measured. Paper surface components such as hydrophobic size [22], wood extractives [23] and fillers [24] lower the delamination force. The negative effects of some surface components can be offset by plasma treatment which introduces polar surface groups [21, 23, 25].

For coated papers, adhesion depends on the nature of the coating materials. Welander [26] showed that the type of binder in the coating has a marked influence on the adhesion of polyethylene to coated paper. For instance, polyethylene displayed a stronger adhesion to paper coating containing styrene-butadiene and CaCO3 pigment than to a coating containing polyvinyl acetate binder and clay pigment.

The influence of paper structure on adhesion

Polyolefin film adhesion to paper is also sensitive to paper structure. Gervason calendared identical paper sheets to different roughness levels before lamination with polyethylene and reported that delamination force increased with increased coating weight and smoothness of paper [21]. The results were interpreted in terms of contact area.

Bikerman [27, 28] was one of the first authors to discuss PSA peeling from paper. He focused on paper as a porous medium and discussed the flow of molten and emulsion adhesives into the paper structure. However, most modern adhesives are too viscous to penetrate into paper. Key observations from Bikerman's work involved the details of the peel force versus peel distance curves. Specifically, he showed that the peel force often reached a maximum value which decayed to a steady-state value. Herein we call this maximum peel force the peak peel force, F_p (N/m). Bikerman also noticed that if a tape was peeled from the edge of a sheet of paper, the peak peel force was lower than if the peeling started away from the paper edge. We have developed a theory to explain this behavior [29], which will be described later.

More than twenty years later, Yamauchi and coworkers [30, 31] reported the first systematic PSA peel studies involving paper properties. They identified three modes of peel failure: interfacial, paper and mixed failure. In the interfacial failure peeling regime, the PSA cleanly separates from the paper surface. A common commercial example of this is the 3M Post-it® note. Yamauchi showed that the mode of peel failure changed from paper failure to interfacial failure by either increasing paper density or decreasing peel rates.

This brief survey of the adhesion science and paper technology literature leads to some general conclusions. First, it is not possible accurately to predict adhesion from first principles and knowledge of adhesive and substrate

compositions. Despite many attempts, semi-empirical surface energy estimates from acid/base models have failed to predict adhesion in many systems [32]. Therefore, although there are exciting experimental innovations in adhesion science including the surface forces apparatus [33], JKR contact mechanics [34] and atomic force microscopy [35], a universal adhesion theory is elusive and practical adhesion remains an empirical science. Furthermore, much of the published adhesion literature involves one-variable-at-a-time studies. This approach is not very useful for adhesion to paper because the inherent complexity of paper makes it next to impossible to change only one property at a time.

Second, there have been very few studies of PSA adhesion to paper in spite of the fact that it is such a pervasive technology. We believe this is because paper is a weak substrate and often fails in conventional adhesion tests giving little information about the PSA adhesion to paper.

This paper summarizes our systematic investigation of PSA peeling from paper. In the following sections we summarize the peeling phenomena and present a new method for analyzing peeling experiments which leads to an outcome we call a peel map. We then apply this analysis to a broad range of papers to yield general conclusions about the influence of paper properties on peeling behaviors. It will be shown that this multivariate statistical approach yields much information. We finish by showing that peeling can be used to estimate paper surface strength.

PEEL RESULTS AND THEIR INTERPRETATION

Typical peeling behaviors

Figure 1 shows curves obtained from peeling a PSA from filter paper at peel angles of 90 and 180 degrees and at both a low and high peel rate. At low peel rate (set A in Figure 1) the adhesive cleanly separated from the paper surfaces leaving no fibre residues in the adhesive – we call this interfacial failure. The corresponding peel curves gave a steady-state peel force which increased with peeling angle. These results are similar to PSA peel curves from a strong substrate such as stainless steel.

By contrast, peeling at higher speed gave more complex behavior (set B in Figure 1). The peel force increased to a maximum and then decreased to a steady-state value. As before, 180 degrees gave greater forces than 90 degrees. High speed peeling resulted in paper delamination.

In previous work we characterized the variability of peel data. Figure 2 shows nine repeated measures of PSA peeling from filter paper [36]. The curve labeled “standard deviation” gives a measure of the variability in the

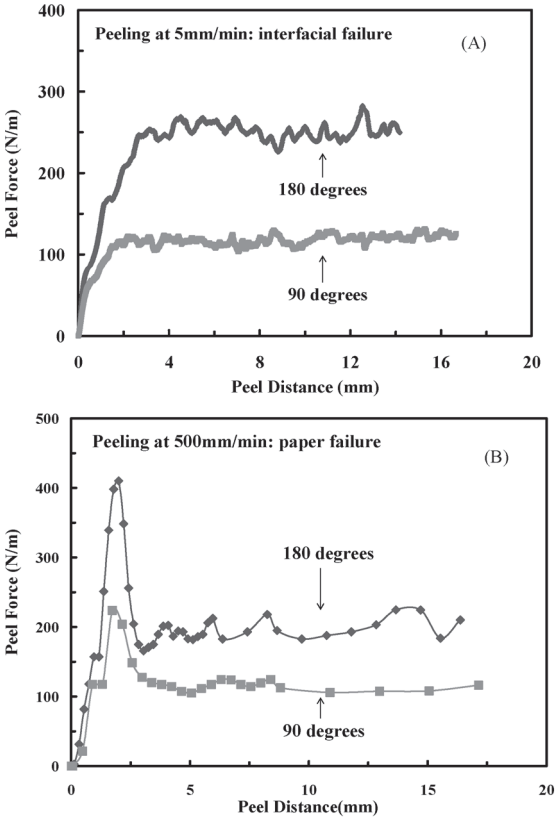

Figure 1 Peeling from Filter paper No. 1(A) at 5mm/min – interfacial failure and (B) at 500mm/min – paper failure.

various stages of peeling. The maximum variability occurred in the transition region when the peel force declined from the maximum value (i.e. the Peak Peel Force, F_p) to the lower steady-state peel force. In this work we used mainly peak peel force values which were simply the maximum values, or the steady-state peel forces, which were determined as the average along a representative segment of the peel curve. For the data in Figure 2, the average peak peel force is 408 N/m and the corresponding standard deviation is 31.6 N/m. The average steady-state peel force is 208 N/m with a standard deviation of 45 N/m.

In our initial attempts to evaluate PSA peeling from paper, we followed the

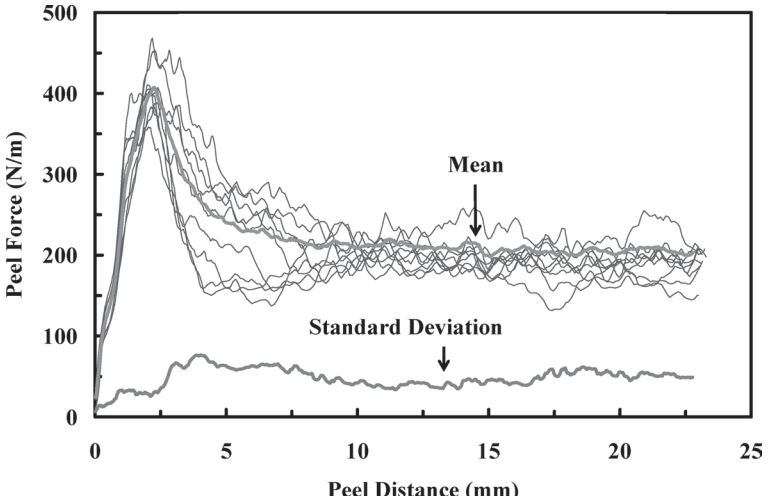

Figure 2 Replicated peel measures of PSA tap 9974B from Whatman No. 1 filter paper. Reproduced with permission [36].

approach described by Yamauchi and coworkers [30, 31] which was to plot steady-state peel force versus peel rate for a series of experiments. Figure 3 shows a typical result. At low peel rates, the failure mode was interfacial and the peel force increased with peel rate. However, at a critical peel rate, V_c, peel force jumped to a lower value giving a discontinuity in the curve corresponding to the onset of paper failure. We attempted to use V_c as a measure of the propensity of a paper to delaminate in peel; however, this approach turned out to be unsatisfactory because it took a great deal of experimentation to achieve accurate values for V_c.

It has been long known that the tendency of a paper to delaminate in peeling can be very sensitive to peeling direction, apparently reflecting whether the fibre ends are orientated up or down in the z-direction, which in turn is a function of the drag-to-rush ratio [38, 39]. Figure 4 shows replicated peeling traces obtained with newsprint at 300mm/min and 400mm/min. One half of the data was obtained by peeling one way in the machine direction (MD1) whereas the other half was peeled in the opposite machine direction (MD2). The MD2 peels all led to paper delamination with a reproducible steady-state peel force. By contrast, the MD1 peels gave reproducible interfacial peel curves with a much higher steady-state peel force. Increasing peel rate from 300mm/min to 400mm/min slightly increased the peak peel forces

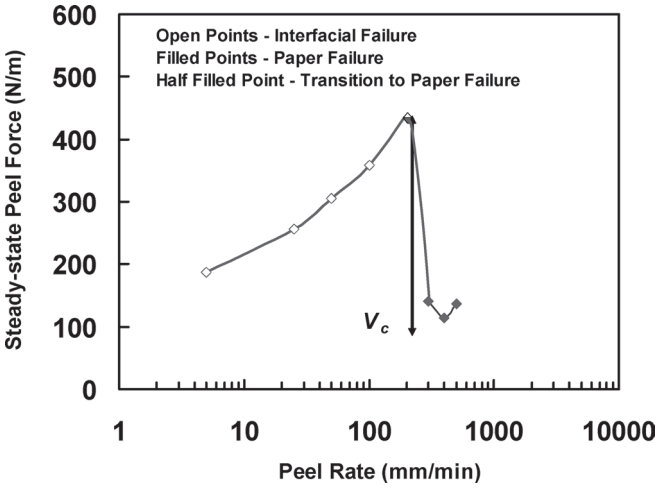

Figure 3 Steady-state peel force versus peel rate. Adapted from [37].

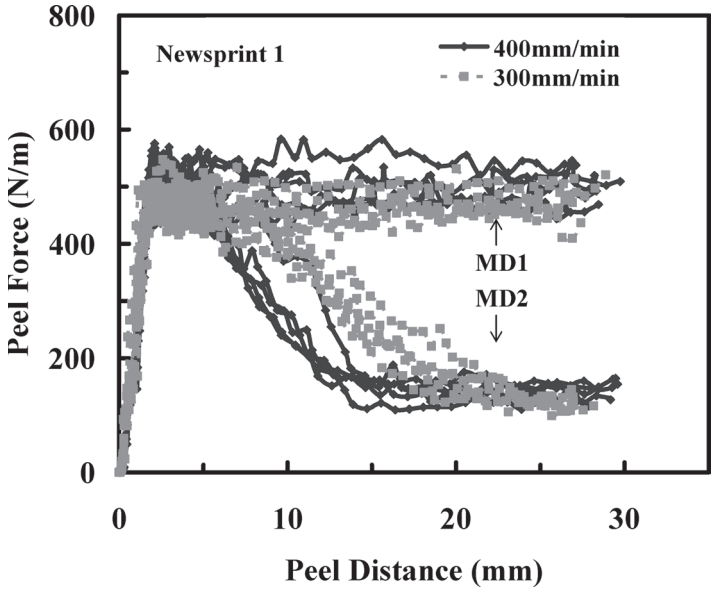

Figure 4 Peeling tape 9974B from Newsprint 1 along two of its machine directions (MD1 and MD2) at 300mm/min (dashed line) and 400mm/min (solid line).

(i.e. the maximum values). The results in Figure 4 are important because they illustrate that although the overall peeling behavior of paper is very complex, the one feature that is independent of peeling direction is the peak peel force. This observation and others led us to formulate a new analysis of peeling curves.

Peel maps – a new method for peel data analysis

Measuring peeling as a function of peel rate is useful because it allows one to observe the transition from interfacial to paper failure. We found that paper-tape interactions are best assessed by conducting a set of peeling experiments at varying peel rates, and plotting the log peak peel forces as a function of the log peel rate [37]. This analysis resulted in what we have called a "peel map" which is illustrated in Figure 5. The peel map consists of two linear segments (on the log/log plots) intersecting when the failure mode changes from interfacial to paper failure. Most paper-tape combinations showed this behavior with the exception of strong papers bonded to weak adhesives, which never gave paper failure.

Three parameters are needed to define two straight lines if one line is horizontal. We chose the peak peel force (F_c) in the paper failure domain (the horizontal line in Figure 5), which is a measure of paper surface strength, the

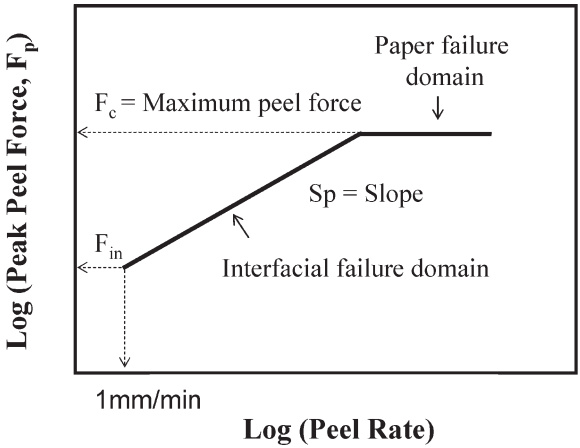

Figure 5 Schematic illustration of a peeling map. The intersection of the two linear segments corresponds to the transition from interfacial failure at low peel rates to paper failure at high rates.

interfacial peel force (F_{in}) at the slow peel rate of 1mm/min, and the slope (Sp) in the interfacial failure domain. By using these three parameters, it is possible to examine the specific linkage between paper properties and the performance of adhesive tape.

Figure 6 shows three peel maps for one type of tape and three filter papers. The slopes of the interfacial failure segments were identical and the curves nearly overlap. On the other hand, the three papers required different peak peel forces to initiate paper failure. This reflects the increase in paper surface strength with density.

By contrast, Figure 7 illustrates the influence of the PSA properties by showing peeling results for three tapes on one paper. The slopes of the interfacial failure regime were sensitive to the type of adhesive. This reflects that fact that much of the peeling energy in the interfacial failure domain is expended on deforming the adhesive. Thus peel force is very sensitive to tape properties. The minimum peel rate required to induce paper delamination was also sensitive to the tape type as a consequence of the varying slopes. On the other hand, the peel force required to initiate paper delamination was independent of the adhesive.

Since our analysis relies on the peak peel force, it is instructive to consider the events causing the maximum peel force. In the case of interfacial failure,

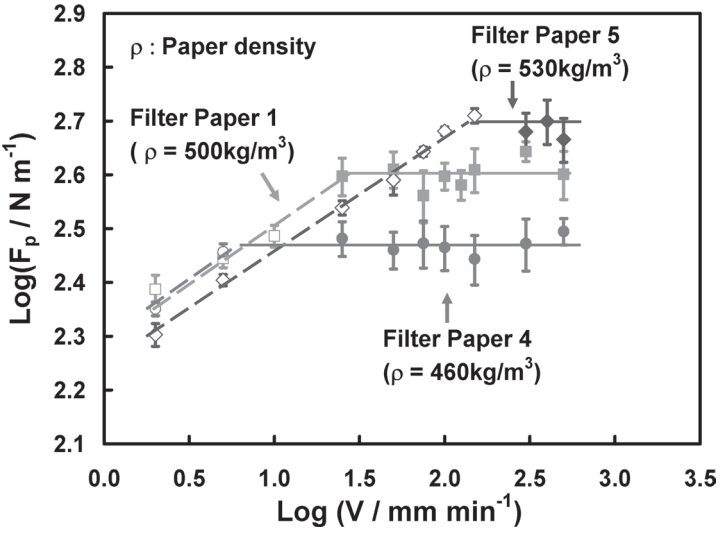

Figure 6 Peeling maps for PSA tape 9974B from three filter papers. Dashed line: interfacial failure; solid line: paper failure.

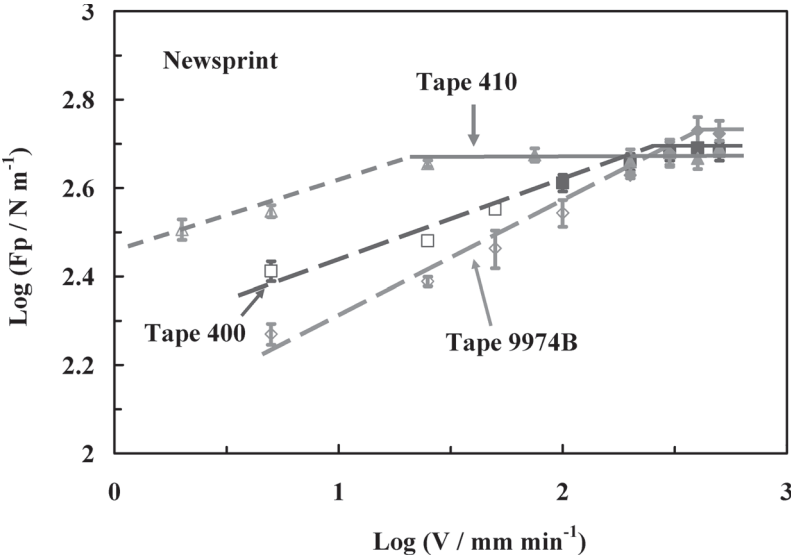

Figure 7 The influence of tape type on the peeling maps for newsprint. Adapted from [36].

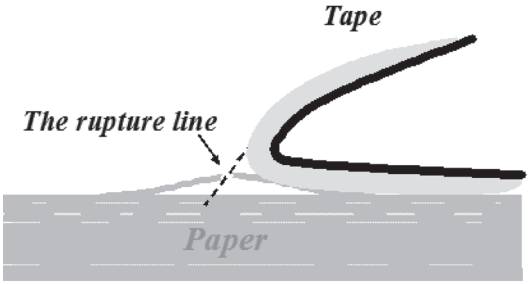

Figure 8 The peak peel force at the initial stages of peeling corresponds to the rupture of the top one or more layers of fibres [29].

the maximum peel force corresponds to steady-state peeling. We will show that the interfacial peel forces are sensitive to paper surface chemistry, roughness and PSA properties. For the more complex paper failure peel curves, such as those shown in Figure 1B, we have shown that the peak peel force corresponds to the fracture of the top one or two layer of fibres – this is illustrated in Figure 8 [29].

THE INFLUENCE OF PAPER PROPERTIES ON TAPE ADHESION

One of our main research goals was to identify the key paper properties influencing tape adhesion. Our initial hypothesis was that PSA peeling behavior was dominated by paper surface chemistry. To test this we treated glassine paper with octyltriethoxylsilane (O-TES). This silane hydrolyzes and polymerizes in the presence of trace water and deposits on the paper surface to give a hydrophobic coating. By varying the silane concentrations and contact time a series of treated glassines was prepared. Figure 9 show the steady-state PSA peel force (interfacial failure domain) as a function of the water contact angle. There was no correlation between peel force and adhesion.

In a second series of experiments, glassines were treated with hydrophobic poly(methylmethacrylate)siloxane (PMMAS) 1500–2000cs, poly(methyl-octyl)siloxane (POMS) 500cs, poly(methylfluoropropyl)- siloxane (PFS) as well as hydrophilic polyethylene glycol (PEG). The results, summarized in Figure 10, show that the hydrophobic polymers greatly increased contact angle with rather minor decreases in peel adhesion. We concluded that the simple one-variable-at-a-time approach could not deal with the complexity of PSA peeling from paper. The following paragraphs summarize results of the

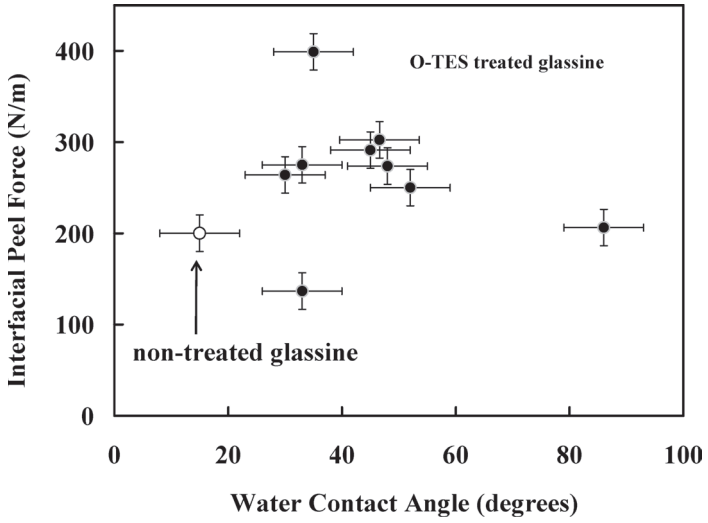

Figure 9 Peel forces versus water contact angles on octyltriethoxylsilane (O-TES) treated glassine papers. Interfacial failure in peeling.

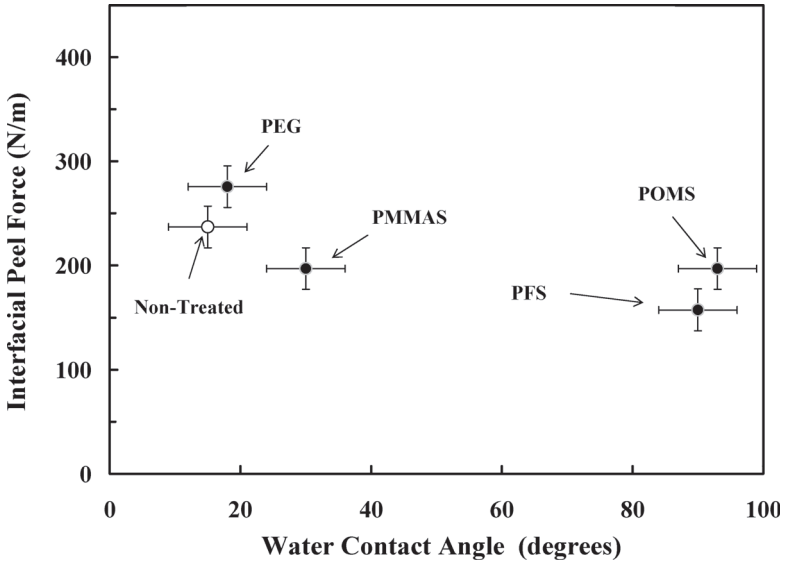

Figure 10 Peel forces versus water contact angle of polymer-modified glassines. Interfacial failure in peeling.

analysis of peeling data from a library of uncoated papers using principal components analysis, a multivariate statistical analysis technique.

A library of uncoated papers was obtained from ASTM, together with a database containing most of the paper properties. Descriptions of papers are given in Table 1 and the complete database together with the details of the statistical analysis was recently published [40]. Most of the fine papers had been prepared on pilot papermachines whereas the newsprint and copy papers were commercial samples

The database of paper physical properties was augmented with two additional data sets. The first additional set was F_c, Sp, and F_{in} (see Figure 5) from the peel maps which, in turn, were obtained by peeling over a series of peel rates. The second set was the paper surface compositions, which were measured by x-ray photoelectron spectroscopy yielding atomic percentages of the various forms of carbon, and other elements.

The principal components analysis generated two new properties for each paper sample, *t1* and *t2*; in the statistical jargon these are called *PCA components*. The new properties, *t1* and *t2*, are linear combinations of the conventional properties. The extent to which each conventional property contributes to the PCA components is governed by a weighting factor, *w*. For

Table 1 Paper samples and their composition. BNSWK denotes bleached softwood kraft, BNHWK bleached hardwood kraft, SW-BCTMP bleached chemithermo-mechnical softwood pulp, HW-BCTMP bleached chemithermomechnical hardwood pulp, SGW stone ground wood, TMP thermomechanical pulp and PCC precipitated calcium carbonate.

Paper sample	Pulp Type 1	Pulp Type 2	Fillers	Internal Size
ASTM paper 1	100% BNSWK	None	None	2#/T Rosin
ASTM paper 2	100% BNSWK	None	5%PCC	None
ASTM paper 4	100% SW-BCTMP	None	5%PCC	None
ASTM paper 5	100% Cotton fiber	None	None	2#/T Rosin
ASTM paper 8	20%BNSWK	8%SLUSH-SGW	5%PCC	None
ASTM paper 9	20%BNSWK	80% HW-BCTMP	None	None
ASTM paper 10	20% BNSWK	80% HaW-BCTMP	5%PCC	None
ASTM paper 11	50% BNSWK	50% BNHWK	None	None
ASTM paper 12	50% BNSWK	50% BNHWK	5%PCC	None
ASTM paper 13	50% BNSWK	50% HW-BCTMP	5%PCC	None
ASTM paper 14	50% BNSWK	50% HW-BCTMP	None	2#/T Rosin
ASTM paper 15	50% BNSWK	50% BNHWK	5%PCC	4#/T AKD
Copy paper 1	–	–	–	–
Copy paper 2	–	–	–	–
Glassine paper	Chemical pulp	None	–	–
Filter paper 1	100% Cotton fiber	None	–	–
Filter paper 4	100% Cotton fiber	None	–	–
Filter paper 5	100% Cotton fiber	None	–	–
Newsprint 1	100% TMP	None	–	–
Newsprint 2	100% TMP	None	–	–
Newsprint 3	100% TMP	None	–	–

Notes:
1 – Most ASTM paper samples were made by the Herty Foundation pilot paper machine except for ASTM paper 5 which was made by Crane & Co. Inc. All these samples were provided through the ASTM Paper-Aging Program.
2 – Copy paper 1 is a commercial copy paper sold by Canon (Ontario, Canada), and Copy paper 2 is Domtar copy paper sold by Domtar (Montreal, Canada). Glassine paper is the commercial Masterpak TM glassine paper #2–11. All newsprint were made and provided by Donohue Inc. in Montreal, Canada. The filter papers 1, 4 and 5 are the commercial Whatman Filters No.1, 4 and 5.

example, tensile strength of the paper contributes to *t1* by a factor of $w1_T = -0.158$ to component t2 by $w2_T = 0.289$. Weightings vary between –1 and +1. In summary, for each paper, there are two new properties, *t1* and *t2*, and each physical property has two new weighting parameters (*w1* and *w2*) which are the extent to which the properties contribute to *t1* and *t2*.

Figure 11 shows the *t2* values plotted against the *t1* values for the 21 paper samples. The various types of papers formed clusters in this plot. For example, the three filter papers were grouped at the right side, while three newsprints were close together at the left side the plot. Thus, Figure 11 shows that the principal components *t1* and *t2* distinguish the different types of papers. However, the most important information comes from the analysis of the corresponding variable weightings.

Figure 12 shows *w2* versus *w1*. Therefore each point in Figure 12 corresponds to one of the conventional paper properties or a peel property or a surface composition property. The rules for interpreting this figure are: 1) variables contributing similar information are grouped together; 2) the impact of a particular variable increases with distance from the origin; and, 3) negatively correlated variables are positioned on opposite sides of the plot origin in diagonally opposed quadrants.

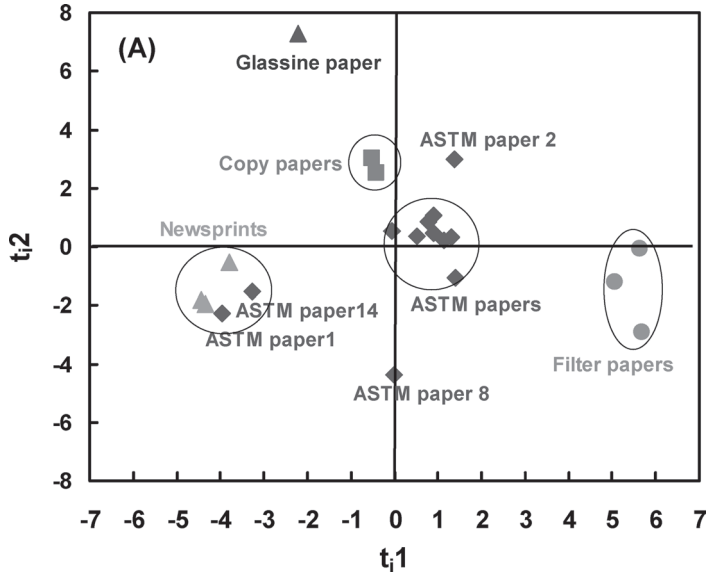

Figure 11 PCA component *t2* versus *t1*. Reproduced with permission [40].

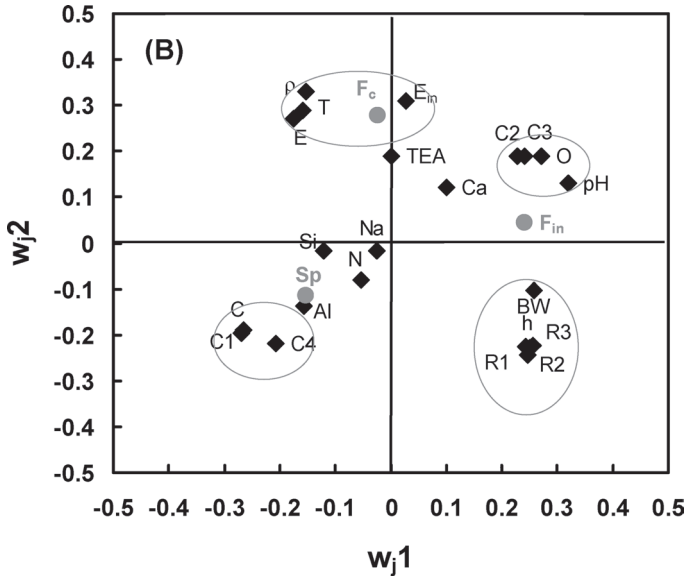

Figure 12 PCA factor *w2* versus *w1*. Reproduced with permission [40].

The weighting parameters approximately fall into four groups of paper properties in Figure 12. The first group consists of tensile strength (T), modulus (E), internal bond strength (E_{in}) and density (ρ), clustered at the top center. The second group consists of percentage of oxygen (O), carbon atoms bound to two oxygens (C2), carbons bound to three oxygens (C3) and surface pH which are clustered at the top right of the plot. Clustered at the bottom right is the third group which consists of the paper basis weight (BW), thickness (h), and three roughness parameters (R1 – the cut-off length of 0.25mm, R2-the cut-off length of 0.8mm and R3-the cut-off length of 2.5mm), The fourth group, clustered at the bottom left, consists of carbon with no (C), one (C1) or four (C4) bonded oxygens. Note that the fourth group of variables is inversely correlated to the second group of O, C2 and C3 which are in the opposing quadrant; and it seems that these two groups could be captured by considering the oxygen/carbon ratio. Finally, the inorganic elements, the content of nitrogen (N) and the total energy adsorption (TEA) are close to the origin indicating they are not important to the analysis.

The three peel responses, F_{in}, F_c and Sp, are not grouped together in Figure 12 indicating they are independent and linked to different paper properties. F_{in} (i.e. the low speed peel force in the interfacial failure domain – see

Figure 5) lies at the right side of the plot origin between the roughness and O, C2, C3 groups, opposite to the group of C, C1 and C4. This implies that F_{in} is sensitive to paper surface chemistry and roughness. By contrast, the maximum peel force, F_c, lies at the top centre of the plot and is grouped with the paper mechanical properties implying that mechanical properties have the major influence on F_c – the relationships between delamination force and other paper properties has been discussed [41, 42, 43]. The slope of the interfacial peel domain, Sp, is closer to the origin of the plot indicating that Sp is less dependent on the paper properties. However, Figure 7 shows that slope is very sensitive to PSA properties.

It was anticipated that paper surface properties would influence peel force in the interfacial failure domain. The statistical analyses confirm that the interfacial peel force is related to both paper surface chemistry and surface roughness. This is illustrated in Figure 13 by plotting F_{in} against the O/C ratio. The O/C ratio, measured by X-ray photoelectron spectroscopy, is used as the indicator of paper surface chemistry, since the oxygen and carbon contents are inversely related. The general trend is that F_{in} increases with the O/C ratio. Indeed this ratio accounts for 50% of the variation of F_{in}.

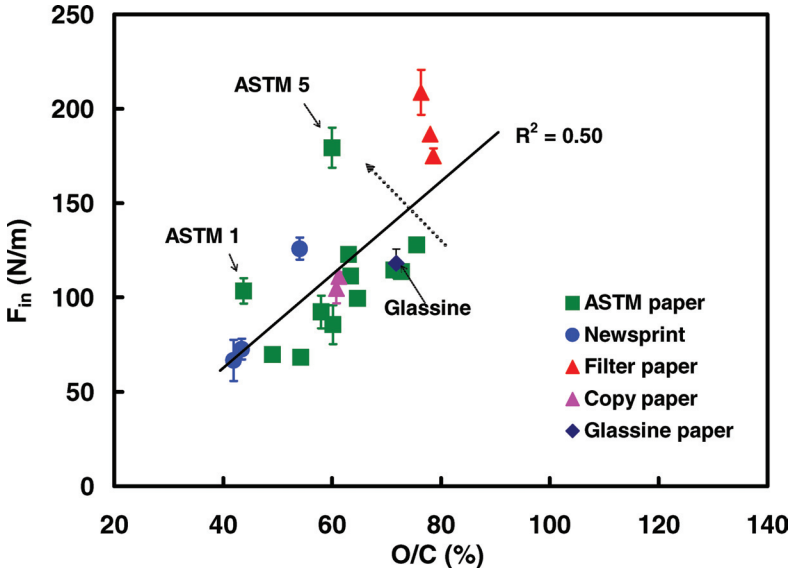

Figure 13 Interfacial peel force F_{in} as a function of O/C, the ratio of surface oxygen to carbon. Reproduced with permission [40].

The O/C ratio can be considered to reflect the relative content of cellulose in the paper surface region. Cellulose with the molecular formula of $(C_6O_5H_{12})_n$ has a high O/C ratio (~0.83), while lignin has a low O/C ratio due to the fact that it consists mainly of aliphatic and aromatic carbons with a few reactive groups such as hydroxyl, carbonyl and carboxyl groups [44]. In addition, paper sizing agents are often added in paper to reduce the ink penetration. Like lignin, such sizing agents are hydrophobic having a very high carbon and low oxygen content from a few functional groups such as carboxyls.

It is interesting to explore further the scattering of the data in Figure 11 by considering a line orthogonal to the correlation line of F_{in} and O/C. For the commercial papers whose roughness displayed significant differences, the smoothest glassine paper lies below that correlation line and the roughest filter papers lie above. It seems that the orthogonal line is related to paper surface roughness; the smoother paper displayed the lower interfacial peel force. For the ASTM samples which display similar roughness, most of them follow the trend line except for two sized samples ASTM 1 and ASTM 5; the origin of this scatter is not known.

Peeling as a measure of paper surface strength

We proposed that the peak peel force could be used as a measure of the paper surface strength when measured at peel rates sufficiently high to initiate paper failure [45]. Figure 14 shows peak peel forces as functions of the industry standard IGT Surface Strength data for the newsprint and ASTM papers. The two methods were correlated for these samples. Peeling offers the advantages of giving a force and requires no qualitative user assessment. Furthermore, the very viscous nature of pressure sensitive adhesives limits their penetration into porous papers.

SUMMARY

The peel map, obtained by plotting log peak peel force versus log peel rate, captures the essential features of PSA peeling from uncoated papers. PSA properties, paper surface composition and, to a lesser extent, surface roughness dominate the interfacial peeling domain, whereas in the peak peel force in the paper failure domain is determined by internal bond and other paper properties linked to surface strength and fibre-fibre bonding.

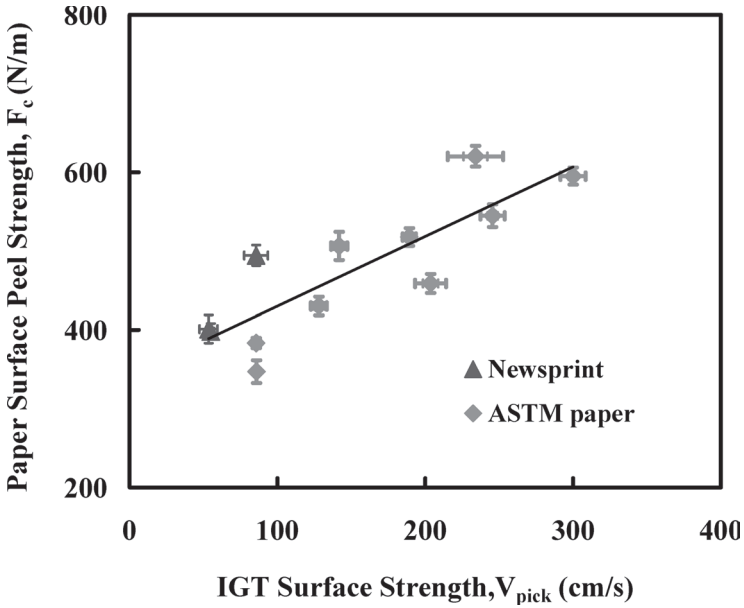

Figure 14 Comparison of paper surface strength by Peel and IGT tests. The error bar shows the standard error of the measurements. Data from [45].

EXPERIMENTAL

The experimental details for the fabrication and peel testing of untreated papers has been described in detail [36]. Detailed descriptions of the paper samples have also been published [40]. For the silane and polymer treatment studies, glassine paper (Masterpak) was treated with n-octyltriethoxysilane (O-TES) 96% from Gelest, or with poly(methylmethacrylate)siloxane (PMMAS) 1500–2000cs, poly(methyloctyl)siloxane (POMS) 500cs, poly-(methylfluoropropyl)-siloxane (PFS) obtained from Petrarch, or with polyethylene glycol (PEG) 1,000 from Aldrich Methyl ethyl ketone (MEK), heptane, ethanol and triethylamine obtained from Aldrich were used as solvents for the chemical treatments.

The tape used for peeling from chemically-treated glassine papers was the 3M Scotch tape No. 411 provided by 3M London. It is a Flexomount¾ printing tape, with adhesive layers coated on both sides of a gray vinyl carrier and with a kraft liner. The thickness of the adhesive layer is 139 μm and the thickness of the vinyl carrier and the paper liner are both 102μm.

Surface modification procedures

Glassine paper strips (23cm × 3cm) were rolled and placed in 20 mL vials containing 10 mL of solution. Excess of chemical agent was removed by dipping the glassine strips three times in fresh solvent. Treated glassine samples were conditioned in the constant temperature/humidity room for 24h before contact angle measurement and peel testing.

For silane treatment, O-TES solutions of 0.2%(w)–60%(w) in MEK were used. Soaking time of the glassine strips in the O-TES solutions varied from 30 min to 60h. The O-TES glassine strips were dried in a vacuum oven at temperatures in the range of 70°C to 100°C and for time periods from 0 to 60h.

For the polymer treatment, the polymers were dissolved in MEK 0.2%(w)–2%(w), and the glassine strips were soaked in the resulting solutions for 30 min.

Water contact angle measurement

The properties of the modified glassine surfaces were probed by measuring the static (advancing) contact angles of 5μL sessile drops at room temperature. Glassine samples were fixed on glass microscope slides by double-sided tape. Contact angles of water were measured by using a NRLCA Goniometer (Ramé-Hart Inc). Each reported value was the average of at least ten independent measurements at different locations on the surface.

Peeling test

180° peel tests according to ASTM D3330–96 were conducted in a constant temperature (23°C) and constant humidity (50%) room. The adhesive-paper laminates were prepared by our standard methods [36] except that the peeling tape was 3M No. 411. The peel rate was 0.5 mm/s. Average peel forces were measured by an Instron automated material tester (Model 4411, Corporation Series IX). At least three samples were tested for each condition.

ACKNOWLEDGEMENTS

This work was supported by 3M Canada and the Natural Science and Engineering Research Council of Canada. We thank 3M Canada for providing many adhesive tapes, Dr. Bruce Arnold (Chair of the ASTM Paper Aging Research Program) for providing pilot machine-made fine paper samples,

Domtar's Donohue Mill for providing newsprint samples, and Dr. Joseph Aspler and Mr. Anthony Manfred for helping with IGT testing on paper surface strength in the Paprican printability laboratory in Montreal, Elaine Miasek, Alison Banks and Luis Anderson for experimental assistance, Anna-Karin Ahlman at the University of British Columbia for helping on fibre length measurement, and Dr. Honglu Yu and Dr. John MacGregor for providing the statistical software and helping on the analysis. Thanks are given to Dr. Mark Kortschot (University of Toronto), Dr. Sören östlund (KTH, Sweden), and Dr. Kaarlo Niskanen (KCL, Finland) for their useful discussions and constructive suggestions on paper physics.

REFERENCES

1. D. Satas. Peel. Ch. 5 in **Handbook of Pressure Sensitive Adhesive Technology** (ed. D. Satas), Van Nostrand Reinhold, 1989.
2. D. W. Aubrey, G. N. Welding, and T. Wong. Failure mechanisms in peeling of pressure-sensitive adhesive tape. *J. Appl. Polym. Sc*i. **13**: 2193–2207,1969.
3. D. H. Kaelble. Theory and analysis of peel adhesion, mechanisms and mechanics. *Trans. Soc. Rheology III* **161**:161–180, 1959.
4. A. N. Gent and X. Y Kaang. Effect of peel angle on peel force. *J. Adhesion* **24**:173–181, 1987.
5. A. El Maachi, S. Sapieha, and A. Yelon. Angle-dependent delamination of paper. part 1: inelastic contribution. *J. Pulp Paper Sci.* **21**(10): 362–366, 1995.
6. A. El Maachi, S. Sapieha, and A.Yelon. Angle-dependent delamination of paper. part 2: determination of deformation and detachment work in paper peeling. *J. Pulp Paper Sci.* **21**(12):401–407, 1995.
7. A. El Maachi, S. Sapieha, and A.Yelon. Angle-dependent delamination of paper. part 3. effect of work of detachment on work of peeling. *Nordic Pulp Paper Res. J.* **14** (1):17–22, 29, 1999.
8. A. Zosel. The effect of fibrillation on the tack of pressure sensitive adhesives. *Int. J. Adhes. Adhes.* **18**:265–271, 1998.
9. A.N. Gent and R.P. Petrich. Adhesion of viscoelastic materials to rigid substrates. *Proc. Roy. Soc.* A**310**:433–448, 1969.
10. S.F. Christensen, H. Everlan, O. Hassager, and K. Almadal. Observations of peeling of a polyisobutylene-based pressure-sensitive adhesive. *Inter. J. Adhes. Adhes.* **18**: 131–137, 1998.
11. J. Du, D. D. Lindeman and D. J. Yarusso. Modeling the peel performance of pressure-sensitive adhesives. *J. Adhesion* **80**:601–612, 2004.
12. K. R. Shull. Contact mechanics and the adhesion of soft solids. *Mat. Sic. and Eng. R.* **36**(1): 1–45, 2002.
13. M. Tirrell. Measurement of interfacial energy at solid polymer surfaces. *Langmuir* 12:4548–4552, 1996.

14. K. L. Johnson, K. Kendall and A. D. Roberts. Surface energy and the contact of elastic solids. *Proc. R. Soc. Lond.* A. **324**: 301–313, 1971.
15. L. Li, M. Tirrell, C. L. Korba and A. V. Pocius. Surface energy and adhesion studies on acrylic pressure sensitive adhesives. *Proc. 24th adhesion society annual meeting* pp274–276, 2001.
16. W. Shen, Y. J. Sheng and I. H. Parker. Comparison of the surface energetics data of eucalypt fibers and some polymers obtained by contact angle and inverse gas chromatography methods. *J Adhesion Sci. Tech.* **13** (8): 887–901, 1999.
17. J.C. Berg. The importance of acid-base interactions in wetting, coating, adhesion and related phenomena. *Nordic Pulp and Paper Res. J.* **1**: 85–94, 1993.
18. J. Borch. Thermodynamics of polymer-paper adhesion: a review. *J. Adhesion Sci. Technol.* **5**(7): 523–541, 1991.
19. J.W. Swanson and J.J. Becher. The adhesion of polyethylene on paper. *Tappi J.* **49**(5): 198–202, 1966.
20. J. Borch. Sizing additives affect on polymer-paper adhesion. *Tappi J.* **65**(2): 72–73, 1982.
21. G. Gervanson, J. Ducom and H. Cheradame. Relationship between surface energy and adhesion strength in polyethylene-paper composites. *British Polymer J.* **21**:53–59, 1989.
22. B. Fredholm and L. Westfelt. New sizing chemicals for improved adhesion in polyethylene extrusion coating of sized paper. *Svensk Papperstldnlng* **7**:201–206, 1979.
23. A. Kempi. Studies on adhesion between paper and low density polyethylene 1influence of the natural components in paper. *Paper and Timber* **78**(10):610–617, 1996.
24. A. Kempi. Studies on the adhesion between paper and low-density polyethylene the influence of fillers. *Paper and Timber* **79**(5):330–338, 1997.
25. D.A.I Goring. Plasma induced adhesion in cellulose and synthetic polymers. *Trans. 5th Fund. Res. Symp.*, (ed. F. Bolam), pp172–201, Ernest Benn Ltd., London, England, 1976.
26. M. Welander. Determination of the adhesion between low density polyethylene and coated paper. *Nordic Pulp and Paper Research J.* **2**: 61–65,1987.
27. J.J. Bikerman. Adhesion to fibrous materials. *Tappi J.* **44**(8):568–571, 1961.
28. J.J. Bikerman and W. Whitney. Peeling tension of paper and paperboard adhints. *Tappi J.* **46**(7):420–424, 1963.
29. B. Zhao and R. Pelton. The Initiation of Tape Peeling Induced Paper Delamination. *J. Pulp Paper Sci.*, **31**(1):33–38, 2005.
30. T. Yamauchi, T. Cho, R. Imarnura, and K. Murakarmi. Peeling behavior of adhesive tape from paper. *Nordic Pulp Paper Res. J.* **3**(3):128–131, 1988.
31. T. Yamauchi, T. Cho, R. Imarnura, and K. Murakarmi. Peeling behavior of film laminated papers. *Nordic Pulp Paper Res. J.* **4**(1):43–47, 1989.
32. J. C. Berg. Semi-Empirical Strategies for Predicting Adhesion, in **Comprehensive Adhesion Science- Surface Science of Adhesion** (ed. A. V. Pocius) pp. 1–75, Elsevier, Amsterdam, 2002.
33. J. Israelachvili. Energy dissipation at the molecular and microscopic levels during

dynamic adhesion processes. *Proc. 26th Adhesion Society Annual Meeting*, pp7–8, 2003.
34. K. R. Shull. Contact mechanics and the adhesion of soft solids. *Mat. Sic. and Eng. R.* **36**(1): 1–45, 2002.
35. A. Paiva, N. Sheller and M.D. Foster. Study of the surface adhesion of pressure sensitive adhesives by atomic force microscopy. *Proc. 22nd Adhesion Society Annual Meeting*, pp412–414, 1999.
36. B. Zhao and R. Pelton. Peel adhesion to paper — interpreting peel curves. *J. Adhesion Sci. Tech.* **17** (6): 815–830, 2003.
37. B. Zhao and R. Pelton. A new analysis of peeling data from paper. *J. Mater. Sci. Lett.* **22**: 265–266, 2003.
38. Derek Page. personal communication.
39. K. Niskanen, I. Kajanto and P. Pakarinen. Paper structure. Ch.1 in **Paper Physics** (ed. K. Niskanen), Fapet Oy, 1998.
40. B. Zhao, L. Anderson, A. Banks and R. Pelton. Paper properties affecting pressure-sensitive tape adhesion. *J. Adhesion Sci. Tech.* **18**(14): 1625–1642, 2004.
41. J. Skowronski and W. Bichard. Fibre-to-fibre bonds in paper. part 1. measurement of bond strength and specific bond strength. *J. Pulp Paper Sci.* **13**(5): 165–169, 1987.
42. J. Skowronski. Fibre-to-fibre bonds in paper. part 2: measurement of the breaking energy of fibre-to-fibre bonds. *J. Pulp Paper Sci.* **17**(6): 217–222, 1991.
43. A. Koubaa and Z. Koran. Measure of the internal bond strength of paper/board. *Tappi J.* **78**(3): 103–111, 1995.
44. E. Sjostrom. Lignin. Ch. 4 in **Wood Chemistry, Fundamentals and Applications**, Academic Press, 1993.
45. B. Zhao and R. Pelton. Using peel as a measure of paper surface strength, *Tappi J.* **30**(7): 3–7, 2004.

Transcription of Discussion

PEELING PRESSURE SENSITIVE TAPE FROM PAPER

Boxin Zhao, Robert Pelton and Vasiliki Bartzoka

Department of Chemical Engineering, McMaster University, Hamilton, Ontario, Canada, L8S 4L7

Richard Kerekes The University of British Columbia

One thing you have not looked at, or I did not note that you did, is the fibre orientation in the paper. In particular, how the fibre orientation is achieved on the paper machine. It can be headbox jet rush or drag, depending on whether the jets are impinging more or less quickly than the wire speed, and these produce different effects. The reason I bring this up is because paper-makers actually use a peel test to determine rush or drag. They place a tape on the paper and pull it one way, then put another tape on it and pull it in the opposing direction. The difference is very large. It is like in your MD1 (the direction of manufacture) or MD2 (180° to the direction of manufacture). I just wondered if you had considered the fibre orientation and the machine conditions anywhere in your test?

Bob Pelton

We have looked at that. We got some sets of fine paper from Domtar where they actually recorded the running direction. So we knew which way the machine orientation was. You see spectacular differences in whether or not you get delamination. The peak peel force does not change much, which I do not understand.

William Sampson University of Manchester

Bob, you have not talked at all about different types of tape.

Discussion

Bob Pelton

We have done work with different adhesives and that is published in one of the adhesion journals. What you see if you use the different types of tapes, is that he horizontal part of the peel map is the same, but the slope and the location of the slanted part, corresponding to interfacial failure varies remarkably. That is because a big part of the interfacial peel force is due to deformation of the adhesive. So, yes we have looked at that.

Patrice Mangin U.Q.T.R./CIPP

The question is about the effect of roughness, which is rather surprising. I also found the same thing with my studies on linting where rough paper linted less. Rough papers showed less fibre removal than the smooth papers. You said that the peel force is actually higher for rough paper. How do you explain that?

Bob Pelton

I do not have a good explanation, but I am an academic, so I can always speculate.

Patrice Mangin

In the case of linting, we could relate the roughness effect to inflow in the printing nip, but you do not have any flow in your experiment.

Bob Pelton

No, Bikerman's analysis treated the paper like a permeable medium and he talked about the adhesive flowing in, but our PSAs (Pressure Sensitive Adhesives) are incredibly viscous. We have looked at penetration in some detail. The adhesives we are looking at do not penetrate at all. PSA remains on the surface. I assume that if paper is rougher perhaps the total contact area is higher.